Available online at www.sciencedirect.com
SCIENCE DIRECT
International Journal of Mass Spectrometry 253 (2006) 38–47
International Journal of Mass Spectrometry
www.elsevier.com/locate/ijms

# The heterogeneous reaction of particle-phase methyl esters and ozone elucidated by photoelectron resonance capture ionization: Direct products of ozonolysis and secondary reactions leading to the formation of ketones

James Zahardis, Brian W. LaFranchi, Giuseppe A. Petrucci *

*Department of Chemistry, University of Vermont, Burlington, VT 05405, USA*

Received 17 January 2006; received in revised form 13 February 2006; accepted 13 February 2006
Available online 24 March 2006

**Abstract**

Photoelectron resonance capture ionization aerosol mass spectrometry (PERCI-AMS) facilitates the measurement of heterogeneous particle-gas phase reactions of relevance to atmospheric chemistry. This methodology, which has been demonstrated to have analytical merit for single component particles, such as oleic acid, has been extended to heterogeneous reactions of binary and ternary particle systems. Herein is described the direct measurement of unambiguous products formed by the reaction between multicomponent particles composed of fatty acids and corresponding methyl esters and ozone. Reaction products measured include unfragmented acids and aldehydes from ozonolysis, in addition to molecular ions of the substrates. The minimal fragmentation afforded by the low energy and tunable photoelectrons unique to the PERCI methodology allows for the straight-forward analysis presented herein. For example, in a reacted three-component particle consisting of methyl oleate/methyl linolenate/methyl linoleate, 25 of the predicted 36 ozonolysis products are measured directly as their molecular ions.

Furthermore, a secondary reaction between in situ-generated Criegee intermediates and unsaturated fatty acids and methyl esters is described leading to the proposed formation of novel ketones. Evidence that this reaction occurs at the carbon–carbon double bond is also presented and a mechanism is proposed. Oxygenation reactions of atmospherically relevant aerosols are of significance in that they may affect particulate properties such as hygroscopicity and ability to act as cloud condensation nuclei.


*Keywords:* Photoelectron resonance capture ionization; Aerosol mass spectrometry; Criegee intermediate; Soft ionization; Ozonolysis

## 1. Introduction

Accounting for the fate of organic carbon in tropospheric processing remains one of the most important problems in atmospheric chemistry today. Atmospheric chemical reactions are often heterogeneous, involving highly reactive trace gases, including, but not limited to OH, $SO_2$, $NO_X$ and ozone and aerosol particles, i.e., liquid- or solid-phase particulate dispersed in air. Analysis and modeling of these reactions lies in part with the complex secondary chemistry that often takes place, generating reactive chemical products that can remain in the condensed phase or be expelled from the particle into the gas phase. Although development of models that can provide insight into the chemical and physical processing of organic particulate phases is underway [1–5], efforts to obtain data necessary to improve existing models have been hampered by the lack of laboratory methods suitable to the detailed chemical study of complex, multicomponent organic particles. The study of simpler heterogeneous reaction systems is therefore a necessary first step to improve understanding of more realistic and environmentally relevant systems. In this respect, studies of the chemical reactions of two-component organic particles and coatings have been initiated [6–11]. The focus of our research is to simulate and study such multicomponent particles by a method developed in our laboratory, photoelectron resonance capture ionization (PERCI) aerosol mass spectrometry (AMS). Herein are reported results obtained by PERCI-AMS in elucidating the chemical products and mechanisms

* Corresponding author. Tel.: +1 802 656 0957; fax: +1 802 656 8705.
*E-mail address:* Giuseppe.Petrucci@uvm.edu (G.A. Petrucci).

1387-3806/$ – see front matter © 2006 Elsevier B.V. All rights reserved.
doi:10.1016/j.ijms.2006.02.010

from the reaction of three-component organic particles with ozone.

Fatty acids are a major class of biogenic organics in the tropospheric particulate [12–21]. As of late, 9-octadecenoic acid (oleic acid) has emerged as a model fatty acid for particle phase reactions with oxidizing gases, most notably ozone [9,10,22–31]. Oleic acid appears to be a good choice for these studies because it has one double bond susceptible to ozonolysis, greatly simplifying the chemical description, and the ozonolysis of alkenes in traditional condensed phases is well characterized [32–34].

Oleic acid is also ubiquitous in both the pristine and polluted troposphere [13,15]. For example, levels of oleic acid on the order of 1 ng $m^{-3}$ have been measured in the remote marine troposphere [13]. Recently, we [26,28,29] and others [9,10,22–25,27,30,31] have made advances in understanding the heterogenous reactions of oleic acid and ozone. In our work, we have directly measured products of secondary reactions of ozonolysis, including 1,2,4-trioxolanes (secondary ozonides) and cyclic geminal diperoxides. We have also directly observed formation of oligomers [29] with masses up to 963 u via reactions of in situ-generated carbonyl oxides, commonly called Criegee intermediates, with the carboxyl groups of oleic acid. These oligomers were proposed to originate from α-acyloxyalkyl hydroperoxides, which dehydrate to the corresponding polyanhydrides. Although there is evidence in the literature of hydroperoxides forming in the oleic acid–ozone system, our work and that of others [6,22] represents the first measurements of how first-generation hydroperoxide products can participate as intermediates in the formation of high molecular weight oligomers. Advances in the chemical understanding of heterogeneous chemistry involving organic particles with oxidizing gases are largely facilitated by the soft ionization afforded by PERCI. This soft and tunable ionization method, when coupled with aerosol mass spectrometry, has proven to be a powerful tool for the investigation of chemical products of heterogeneous reactions on aerosol particles.

The work described herein is a description of the reaction of two multicomponent organic particles: oleic acid/methyl palmitate and methyl oleate/methyl linoleate/methyl linolenate with ozone. Described herein are the products of ozonolysis that are directly observed by PERCI-AMS and elucidation of a secondary reaction involving the cycloaddition of the unsaturated methyl esters (and corresponding fatty acids) with a Criegee intermediate. We propose that this secondary reaction leads to increases in the oxygen content of atmospheric particulate by formation of ketones in the processed particles. A mechanism for this reaction is proposed.

This work is significant in that it represents, to our knowledge, the direct observation of product evolution in a heterogeneous reaction system with a multicomponent particle phase, including products associated with secondary reactions. Furthermore, the existence of this recently observed oxidation pathway may impact aerosol chemistry models being developed insofar as changes in oxidative states of the organic compounds will affect the hygroscopicity of the reacted particles.

## 2. Experimental

### 2.1. Photoelectron resonance capture ionization aerosol mass spectrometer

A detailed description of the PERCI-AMS has been published previously [28,35], however some modifications have been made. Briefly, aerosol particles are introduced into the mass spectrometer through a differentially pumped inlet and focused into a beam using an aerodynamic lens. A 220 μm diameter critical orifice at the entrance of the inlet keeps the aerosol sampling flow rate constant at 0.45 L/min. The ionization source consists of a low energy (sub-mJ) pulsed (10 Hz), tunable (235–300 nm) ultraviolet laser (Opotek Inc., Carlsbad, CA) focused gently onto the surface of a pure aluminum photocathode, generating a short (7 ns) burst of photoelectrons. For all results presented here, the laser wavelength was fixed at 270 nm. A vaporization probe is placed in close proximity (∼1 cm) to the photocathode and intercepts the particle beam. Vaporization and analysis is done after collecting sampled aerosol on the vaporization probe (at room temperature) for a short time, $t_{dep}$. Mass analysis of the PERCI anions is achieved with a time-of-flight mass spectrometer (R. M. Jordan, Inc., Grass Valley, CA) operating in reflectron mode. Data is acquired at 1 GS/s using a digital oscilloscope (WavePro 7000, LeCroy, Chestnut Ridge, NY). A trigger condition is set to save each laser shot in which an ion signal is detected within a given mass range (100–500 *m/z* in these experiments).

A significant change has been made to the vaporization source from that reported in previous publications [28,35], incorporating temperature measurement and control. The new vaporization probe consists of a resistively heated nichrome filament wrapped around a heat-conducting ceramic cylinder (radius ∼2 mm, length ∼4 mm) constructed from Resbond 919 electrically resistant ceramic adhesive (Cotronics Corp, Brooklyn, NY). Embedded into the heat-conducting ceramic is a type-k thermocouple junction. A CN8201 series Omega (Stamford, CT) temperature controller is used to monitor the temperature of the ceramic and to control the current applied to the filament. A maximum temperature of 400 °C is accessible with this source, well above the atmospheric pressure boiling points of the compounds studied. A temperature ramp from 40 to 385 °C over the course of 1 min is used for these experiments, though in most cases the major components have been completely vaporized by the time the vaporizer reaches 200 °C, which takes approximately 20 s. There is some delay in transferring the heat from the filament to the ceramic, due to the larger thermal mass of the ceramic cylinder. Therefore, the temperature measured by the thermocouple embedded in the ceramic will lag the temperature of the filament, especially during a quick temperature ramp. The result is a quick burst in signal at the very beginning stages of the temperature ramp, presumably, as the deposited aerosol components that are in direct contact with the filament are vaporized first. The remaining deposited aerosol then vaporizes as the temperature of the ceramic cylinder increases.

Table 1
Experimental conditions used in recording mass spectra in this work

| Figure | Analyte | Mole fraction | $P_{ozone}$ (atm) | $t_{rxn}$ (s) | $t_{dep}$ (min) | Averaging | Temperature range (°C) | Smoothing |
|---|---|---|---|---|---|---|---|---|
| 1 | MP:OL | 0.53:0.47 | $1.4 \times 10^{-4}$ | 30 | 2 | 17/17 | 40–380 | No |
| 2 | MO:MLN:ML | 0.33:0.34:0.33 | $1.0 \times 10^{-4}$ | 46 | 5 | 9/33 | 40–175 | Yes |

### 2.2. Particle generation and flow reactor

Fatty acid and ester particles are produced by nebulization (concentric pneumatic nebulizer, J.E. Meinhard Associates, Santa Ana, CA) of a dilute solution of the analyte in 15% ethanol in water. The analytes used are methyl palmitate (MP), oleic acid (OL), methyl oleate (MO), methyl linoleate (ML), and methyl linolenate (MLN). The solution concentrations of MP and OL for the binary particle experiments were $1.78 \times 10^{-3}$ and $1.58 \times 10^{-3}$ M, respectively, yielding particles with an MP:OL mole fraction of 0.53:0.47. The analyte solution concentrations for the ternary particle were $2.95 \times 10^{-3}$ M (MO), $3.06 \times 10^{-3}$ M (MLN) and $3.02 \times 10^{-3}$ M (ML). The M0:MLN:ML mole fractions in the desolvated particles were 0.33:0.34:0.33. The particles are introduced to a flow reactor via a glass tube (0.32 cm ID), centered within a 2.54 cm ID flow reactor, which acts as the aerosol injector. Ozone is generated by passing USP medical air (Airgas Inc.) through an electric discharge ozonator (Model 8340, Mathesen). The concentration of ozone is determined spectrophotometrically by passing the air–ozone mixture through a 10.0 cm quartz cell (NSG Precision Cells, Inc., Farmingdale, NY) that is in line with a magnesium hallow cathode lamp and an echelle polychromator (ESA 3000, LLA Instruments GmbH, Berlin-Adlershof, Germany). Absorption of radiation at the 279.55 nm emission line of magnesium by ozone ($\sigma = 415.8 \times 10^{-20}$ cm$^2$) is used to determine the partial pressure of ozone flowing through the cell. The ozone is introduced into the flow reactor (2.54 cm ID) upstream of the aerosol injector. The flow of the gas is laminar ($Re < 100$) at one atmosphere total pressure within the flow reactor. The ozone exposure time for the particles is dictated by the position of the aerosol injector at a given flow rate of the particle and gas phases.

Table 1 gives the experimental details for each mass spectrum referenced in this work. $P_{ozone}$ is the measured partial pressure of ozone in the flow reactor. The time of exposure of the particles to ozone is given as $t_{rxn}$, while the collection time of particles on the vaporization probe is given as $t_{dep}$. Each mass spectrum referenced is an average of a series of single shot spectra collected during a particular collection and vaporization cycle. The number of spectra averaged and the total number of spectra saved for each experiment is given in Table 1. Also included is the temperature range over which the spectra contributing to the average were collected. Finally, some spectra were processed using an adjacent point average (10 points); it is noted in Table 1 where smoothing was applied. This degree of smoothing does not compromise the mass spectral resolution.

## 3. Discussion

### 3.1. Establishing ionization trends of particle phase analytes

In a prior work [35] we have shown that PERCI proceeds by both associative and dissociative electron attachment (AEA and DEA, respectively) mechanisms. This trend is held with fatty acids and their methyl esters and is presumed to be mediated by the loss of hydrogen from the carboxyl group of the acid. Similarly, ionization of the methyl ester analogues may proceed through loss of the methyl group, which, as discussed below, may lead to some ambiguity in ion identification in a few cases. Herein we give an empirical description of the PERCI of a model methyl ester:methyl palmitate (MP).

As detailed above, methyl palmitate was introduced into the flow reactor as a mixed particle along with oleic acid (OL). Oleic acid served as an internal standard for calibration since its ozonized and non-reacted mass spectra and its PERCI response are well established in our group [26,28,29]. Methyl palmitate contains no alkene moiety, eliminating potential complications in our initial attempts to describe ionization of a methyl ester by PERCI or PERCI coupled with ozonolysis. Under the aforementioned experimental conditions for assaying the effects of PERCI on MP/OL mixed particles, a medium intensity signal was observed at 269 $m/z$ (Fig. 1). We assign this signal, which was absent from all prior studies with oleic acid, to the DEA ionization of MP, i.e., $[MP–H]^-$. Another peak of medium intensity

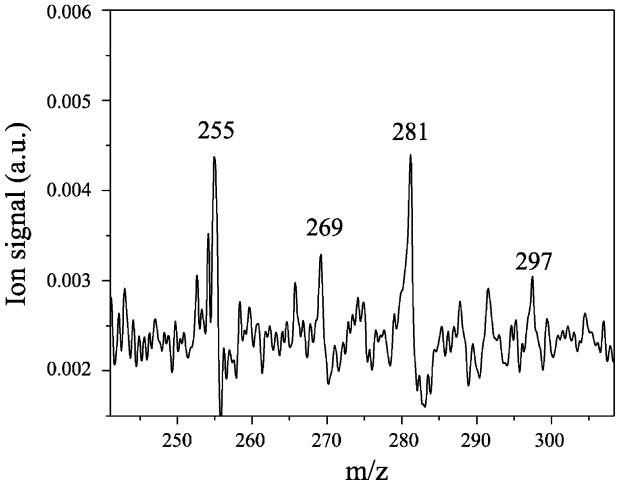


Fig. 1. Portion of PERCI mass spectrum of mixed particle of oleic acid and methyl palmitate after reaction with $O_3$. Experimental conditions given in Table 1.

Table 2a
Molecular formulas for all analytes used in this study: MO (methyl oleate), MLN (methyl linolenate), ML (methyl linoleate), and their corresponding fatty acids

| Name | Formula | MW (u) | *m/z* | Ion signal |
|---|---|---|---|---|
| 9,12,15-Octadecatrienoic acid (linolenic acid) | $CH_3CH_2CH=CHCH_2CH=CHCH_2CH=CH(CH_2)_7CO_2H$ | 278 | 277 | W |
| 9,12-Octadecadienoic acid (linoleic acid) | $CH_3(CH_2)_4CH=CHCH_2CH=CH(CH_2)_7CO_2H$ | 280 | 279 | W |
| 9-octadecenoic acid (oleic acid) | $CH_3(CH_2)_7CH=CH(CH_2)_7CO_2H$ | 282 | 281 | W |
| Methyl 9,12,15-octadecatrienoate (methyl linolenate) | $CH_3CH_2CH=CHCH_2CH=CHCH_2CH=CH(CH_2)_7CO_2CH_3$ | 292 | 291 | VW |
| Methyl 9,12-octadecadienoate (methyl linoleate) | $CH_3(CH_2)_4CH=CHCH_2CH=CH(CH_2)_7CO_2CH_3$ | 294 | 293 | VW, B |
| Methyl 9-octadecenoate (methyl oleate) | $CH_3(CH_2)_7CH=CH(CH_2)_7CO_2CH_3$ | 296 | 295 | VW |

VW-very weak, $\leq$1% $I_{bp}$; W-weak, 1% < $I_{bp}$ < 5%; M-medium, 5% < $I_{bp}$ < 10%; S-strong, >10% $I_{bp}$; $I_{bp}$ is the intensity of the base peak (73 *m/z* for propanoic acid); B-broad, >2 Da base peak width.

is observed at 255 *m/z*, which we assign to palmitate ($P^-$). The palmitate may be generated in situ through thermal [36] and/or optical [37,38] mechanisms, through the PERCI-DEA process, or may be an impurity in the methyl ester sample. While it may be interesting to determine the precise source(s) of acids in the ester samples, the sources are not important to the ensuing discussions.

The general characterization of the ionization of esters, including methyl esters, by PERCI is being investigated in our laboratory currently. For the ensuing discussion involving reaction of a ternary particle composed of methyl esters, the observation of ionization by DEA and ions that are the carboxylates corresponding to their respective methyl esters is in good agreement with our preliminary results.

### *3.2. The ozonolysis of ternary particles of methyl esters: direct observation of primary products*

As described in an earlier work, [26] ozonolysis of an unsaturated organic molecule, such as oleic acid, results in products associated with the decomposition of a 1,2,3-trioxolane (i.e., primary ozonides). These products are typically aldehydes or carboxylic acids under oxidative conditions [34,39] and for this work shall be referred to as primary products. In this section, the primary products of ozonolysis of methyl esters and their corresponding carboxylic acids shall be described.

The ternary particles used for this study were composed of methyl oleate (MO), methyl linoleate (ML), and methyl linolenate (MLN). The molecular formulas for these methyl esters, their corresponding acids, and measured DEA ion signal masses are given in Table 2a. The complete PERCI mass spectrum of a mixed particle of MO, ML, and MLN is shown in Fig. 2a–d. In terms of anticipated ozonolysis products, methyl oleate should be the simplest of the three methyl esters assayed. Fig. 2c shows a medium intensity signal at 295 *m/z* for the molecular ion of MO. This is in concert with the DEA observed in our preliminary studies with the binary MP/OL system. The oleate, $[OL–H]^-$, is assigned to the signal at 281 *m/z*. Also evident in Fig. 2 are other products associated with ozonolysis of MO including the ac-route products: 9-methoxy-9-oxononanoic acid (202 u), and nonanal (142 u); as well as bc-route products: methyl 9-oxononanoate (186 u) and nonanoic acd (158 u). It should be noted that the ion signal at 281 *m/z* can also arise from partial ozonolysis of MLN, as depicted in Fig. 3.

The differences of ion intensity for a given decomposition route can be rationalized by considering several factors. Consider the stronger signal intensity of the 201 *m/z* ion, due to 9-methoxy-9-oxononanoic acid ($HO_2C(CH_2)_7CO_2CH_3$), compared to the other MO ac-route ion at 141 *m/z* (Fig. 2b). The *m/z* 201 signal is approximately a factor of 10 greater than that at *m/z* 141. Nonanal can be formed by only two oxidative cleavage routes in this ternary system, namely the ac-cleavage of MO and a similar cleavage of the OL. On the other hand, there exist 13 independent channels by which the 201 *m/z* ion can be formed. It should be noted that the 201 *m/z* ion, which can be formed by both partial and complete ozonolysis, can also be formed by channels from MLN and ML in addition to MO. We have also observed in earlier studies of oleic acid that the ion signals are generally stronger for acids than for aldehydes under analogous experimental conditions, most likely due to a greater sensitivity of PERCI toward the acid moiety. In addition, the higher vapor pressure of nonanal may also contribute to its lower overall ion signal due to evaporative losses during particle collection onto the probe. These factors may explain, in part, the greater ion signal of 9-methoxy-9-oxononanoic acid compared to nonanal. Similar arguments with regard to the number of channels of ion formation, differences in PERCI sensitivity (i.e., ion formation efficiency) and vapor pressure can be used to explain many of the observed differences in ion intensity for a given cleavage route pair.

In terms of ozonolysis, methyl linoleate presents a more complicated substrate compared to methyl oleate due to its two double bonds. Methyl linoleate can be cleaved at just one double bond, i.e., partial ozonolysis, or be completely ozonized, undergoing oxidative cleavage at both double bonds. We observe ions associated with both extents of ozonolysis in the PERCI mass spectrum (Fig. 2c and d), depending on total reaction time. The ML DEA molecular ion (293 *m/z*) appears as a very weak signal, while the ion signal at 291 *m/z* is assigned to MLN. The molecular ion formed by DEA of the corresponding linoleic acid (L) is clearly observed as a medium–weak intensity ion signal at 279 *m/z* (Fig. 2c). In addition to the molecular ions of ML and L, there are only three other DEA ions that can stem *solely* from these species by direct decomposition of their corresponding 1,2,3-trioxolanes. These ions are at 155, 139, and 99 *m/z*. All of the remaining ions can originate from MLN, MO, LN, and OL. Notice the 155 *m/z* product, proposed to be the DEA ion of non-3-enoic acid, is much lower in intensity than neighbouring ions at 153 and especially 157 *m/z*. The non-3-enoic acid can only

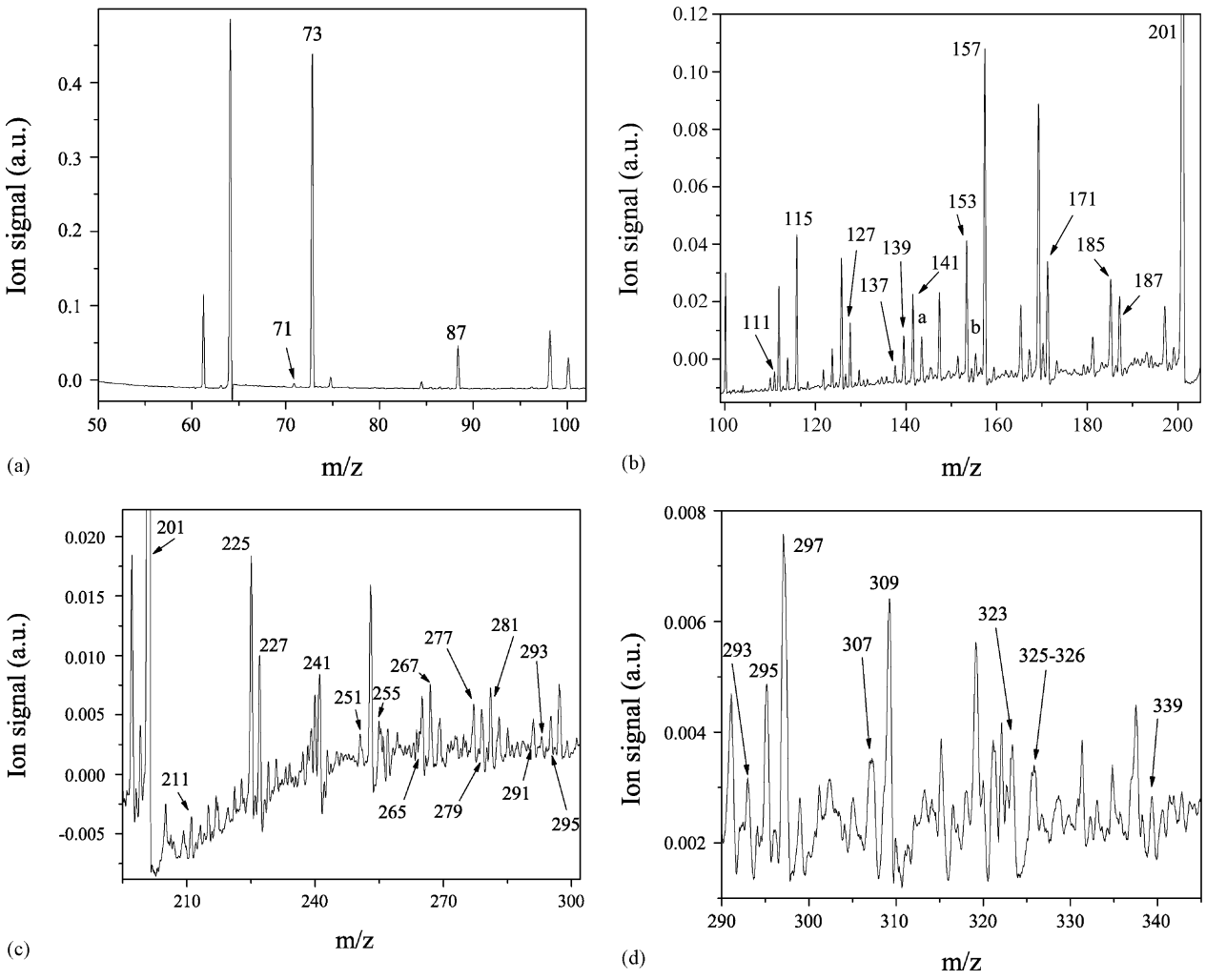


Fig. 2. Complete PERCI mass spectrum for the mixed ternary particle MO/MLN/ML after reaction with $O_3$.The spectrum has been divided into 4 parts (a–d) to permit qualitative comparison of relative ion signal strengths. The peaks designated "*a*" and "*b*" in part (b) correspond to 143 and 155 *m/z*, respectively. The absolute signal intensity for the *m/z* 201 signal (parts (b) and (c) is 0.452). The signal-to-noise ($1\sigma$) of the *m/z* 297 peak is 13. Note different scales of ordinate. Experimental conditions given in Table 1.

arise from the bc-cleavage at the 9-position of ML and L, and is formed with one double bond remaining susceptible to ozonolysis. On the other hand, nonanoic acid (157 *m/z*) is not susceptible to further ozonolysis, which may explain, in part, its greater ion intensity. The case between the 153 *m/z* ion and the ion arising from non-3-enoic acid is not immediately clear: the former ion arises from nona-3,6-dienoic acid, which has two double bonds that are susceptible to ozonolysis. Notice that non-3-enoic acid can be further oxidized, forming primary products with masses at 116, 104, 100, and 88 u. A unique ion originating from ML/L is observed at 139 *m/z* and is likely the DEA product of non-3-enal, which can be formed only by the ac-route cleavage of the 9-position of ML or L. A summary of the remaining products, which could arise from ML/L along with other methyl esters and corresponding fatty acids are summarized in Table 2b.

Methyl linolenate and linolenic acid, through possessing three double bonds susceptible to ozonolysis, potentially can form many more products than MO/OL and ML/L. Nonetheless, ozonolysis of these compounds still forms products and ions by similar mechanisms described previously. Only a brief discussion of the most salient features of the ozonolysis of MLN/LN follows; however, a complete listing of all the primary products of ozonolysis are listed in Table 2b.

The DEA molecular ions of MLN/LN are clearly evident in Fig. 2c at 291 and 277 *m/z*, respectively. Products that are unique to MLN and LN are: Methyl 15-oxopentadeca-9,12-dienoate (265 *m/z*); pentadeca-3,6-dienedioic acid (267 *m/z*); 15-oxopentadeca-9,12-dienoic acid (251 *m/z*); nona-3,6-dienal (137 *m/z*); 6-oxohex-3-enoic acid (127 *m/z*); hex-3-enoic acid (113 *m/z*); hex-3-enedial (111 *m/z*); hex-3-enal (97 *m/z*); propanoic acid (73 *m/z*); and propanal (57 *m/z*). The higher *m/z* signals (251, 265, and 267) are also clearly evident.

Most of the lower *m/z* signals associated with ions arising solely from ozonolysis products of MLN/LN are less intense than their higher *m/z* congeners. The 137 *m/z* signal from nona-3,6-dienal is seen in Fig. 2b as well as the signal at 127 *m/z*; formed from DEA of 6-oxohex-3-enoic acid. The 111 *m/z* ion assigned to hex-3-enedial is evident in Fig. 2b, however, the expected ion signals at 97 *m/z* from hex-3-enal and the 57 *m/z*

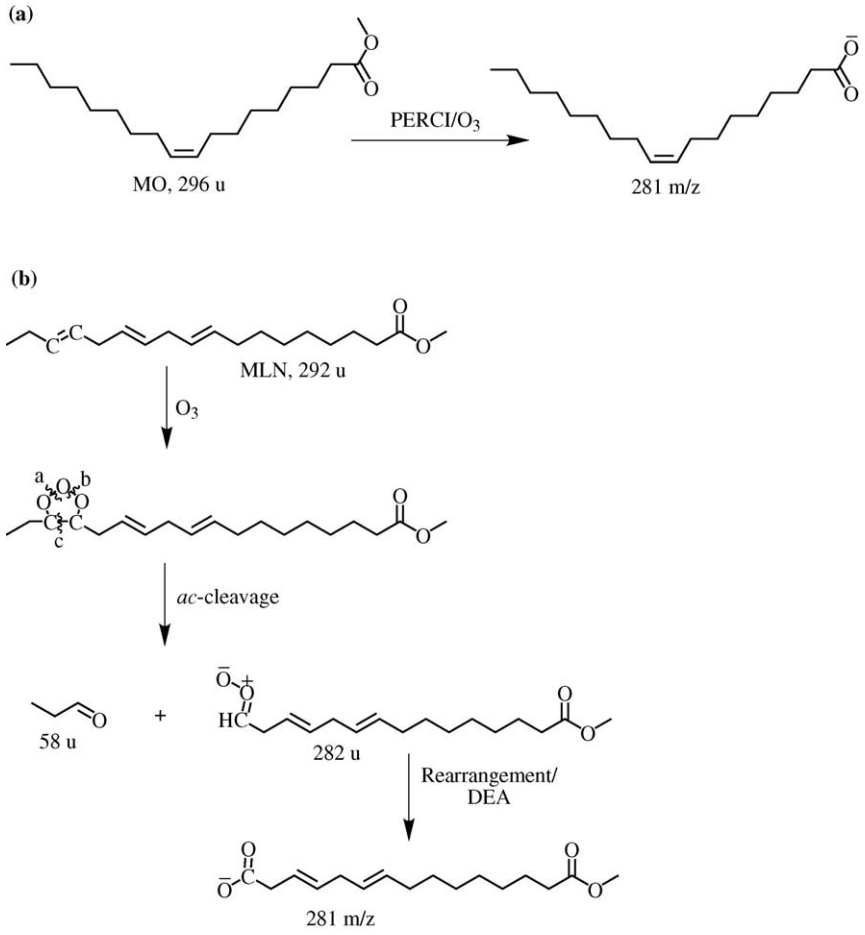


Fig. 3. Two pathways proposed for generation of the 281 *m/z* ion observed by PERCI-AMS: (a) a pathway directly from methyl oleate, induced by ozonolysis or PERCI-ozonolysis; (b) a pathway through methyl linolenate.

from propanal are absent, likely due to their rather high vapor pressure. Ions that can be formed from MLN/LN as well as ML/L and/or MO/OL are summarized in Table 2b.

There are 30 primary products of ozonolysis for this ternary system and six molecular ions for the methyl esters and corresponding fatty acids. Of these 36 products, 25 are clearly discernable from the baseline and have been assigned intensities ranging from weak (W) to strong (S) as defined in Table 2a and b. Peaks defined as very weak (VW) or broad (B), although assigned tentatively, were not considered in the total of 25. Five predicted peaks are not observed above the instrumental noise (57, 97, 99, 103 and 113 *m/z*); however, the 69 and 71 *m/z* signals may arise from decarboxylation and DEA of hex-3-enoic acid (114 u) and hexanoic acid (116 u). The remaining anticipated primary products of ozonolysis are ambiguous, reported as very weak or broad, as summarized in Table 2b.

### *3.3. The dipolar ophilic reaction of unsaturated methyl esters and in situ-generated fatty acids leading to ketone formation*

In a prior work [29] we described the formation of a molecular ion at 297 *m/z* in the oleic acid–ozone heterogeneous reaction system. We assigned this signal to 9 or 10-oxooctadecanoic acid. This was in accord with a model of cycloaddition–decomposition proposed by Katrib et al. [27] in an independent work. These workers described a cycloaddition of a Criegee intermediate (as a biradical) with the double bond of oleic acid, which, upon decomposition, lead to oxooctadecanoic acid. Our mechanism was similar except we showed it via a zwitterionic Criegee intermediate for reasons discussed in that work. Herein we present further evidence of the novel formation of a ketone, where the carbon–carbon double bond of an unsaturated methyl ester or fatty acid acts as a dipolarophile towards a Criegee intermediate. Furthermore, we provide evidence that polyunsaturated methyl esters and fatty acids may undergo multiple cycloaddition–decomposition cycles, thereby increasing the oxygen content of the organic particles that are exposed to ozone.

To test our hypothesis that the increase in *m/z* corresponding to 16 Da stems from oxygenation about the carbon–carbon double bond, we assayed a mixed particle with equimolar concentrations of oleic acid and stearic acid (S) (PERCI mass spectrum not shown); the latter at 284 u being the saturated analogue of the former. Unreacted oleic and stearic acids produced molecular ions of the same intensity (within 5%), indicating no significant measurement bias from the PERCI process. After ozonolysis of the equimolar OL/S particles, a medium intensity

Table 2b
Predicted first-generation chemical products from the ozonolysis of MO, ML, MLN, and other corresponding fatty acids

| Name | Formula | MW (u) | *m/z* | Ion signal |
|---|---|---|---|---|
| Propanal | $CH_3CH_2CHO$ | 58 | – | – |
| Malonaldehyde | $HOCCH_2CHO$ | 72 | 71 | VW |
| Propanoic acid | $CH_3CH_2CO_2H$ | 74 | 73 | Base |
| 3-Oxopropanoic acid | $HO_2CCH_2CHO$ | 88 | 87 | VW |
| Hex-3-enal | $CH_3CH_2CH=CHCH_2CHO$ | 98 | – | – |
| Hexanal | $CH_3(CH_2)_4CHO$ | 100 | – | – |
| Malonic acid | $HO_2CCH_2CO_2H$ | 104 | – | – |
| Hex-3-enedial | $HOCCH_2CH=CHCH_2CHO$ | 112 | 111 | W |
| Hex-3-enoic acid | $CH_3CH_2CH=CHCH_2CO_2H$ | 114 | – | – |
| Hexanoic acid | $CH_3(CH_2)_4CO_2H$ | 116 | 115 | M |
| 6-Oxohex-3-enoic acid | $HOCCH_2CH=CHCH_2CO_2H$ | 128 | 127 | W |
| Nona-3,6-dienal | $CH_3CH_2CH=CHCH_2CH=CHCH_2CHO$ | 138 | 137 | W |
| Non-3 -enal | $CH_3(CH_2)_4CH=CHCH_2CHO$ | 140 | 139 | W |
| Nonanal | $CH_3(CH_2)_7CHO$ | 142 | 141 | M |
| Hex-3-enedioic acid | $HO_2CCH_2CH=CHCH_2CO_2H$ | 144 | 143 | W |
| Nona-3,6-dienoic acid | $CH_3CH_2CH=CHCH_2CH=CHCH_2CO_2H$ | 154 | 153 | S |
| Non-3-enoic acid | $CH_3(CH_2)_4CH=CHCH_2CO_2H$ | 156 | 155 | W |
| Nonanoic acid | $CH_3(CH_2)_7CO_2H$ | 158 | 157 | S |
| 9-Oxononanoic acid | $HOC(CH_2)_7CO_2H$ | 172 | 171 | M |
| Methyl 9-oxononanoate | $HOC(CH_2)_7CO_2CH_3$ | 186 | 185 | M |
| Azelaic acid | $HO_2C(CH_2)_7CO_2H$ | 188 | 187 | M |
| 9-Methoxy-9-oxononanoic acid | $HO_2C(CH_2)_7CO_2CH_3$ | 202 | 201 | S |
| 12-Oxododec-9-enoic acid | $HOCCH_2CH=CH(CH_2)_7CO_2H$ | 212 | 211 | W |
| Methyl 12-oxododec-9-enoate | $HOCCH_2CH=CH(CH_2)_7CO_2CH_3$ | 226 | 225 | W |
| Dodec-3-enedioic acid | $HO_2CCH_2CH=CH(CH_2)_7CO_2H$ | 228 | 227 | W |
| 12-Methoxy-12-oxododec-3 -enoic acid | $HO_2CCH_2CH=CH(CH_2)_7CO_2CH_3$ | 242 | 241 | W |
| 15-Oxopentadeca-9,12-dienoic acid | $HOCCH_2CH=CHCH_2CH=CH(CH_2)_7CO_2H$ | 252 | 251 | W, B |
| Methyl 15-oxopentadeca-9,12-dienoate | $HOCCH_2CH=CHCH_2CH=CH(CH_2)_7CO_2CH_3$ | 266 | 265 | W |
| Pentadeca-3,6-dienedioic acid | $HO_2CCH_2CH=CHCH_2CH=CH(CH_2)_7CO_2H$ | 268 | 267 | W |
| 15-Methoxy-l 5-oxopentadeca-3,6-dienoic acid | $HO_2CCH_2CH=CHCH_2CH=CH(CH_2)_7CO_2CH_3$ | 282 | 281 | W |

Assignments made in analogous manner to those for ozonolysis products in Table 2a.

peak was measured at 297 *m/z* ($[OL-H+O]^-$); however, only a very weak signal was observed at 299 *m/z*, which would be indicative of the $[S-H+O]^-$. Note that in a prior publication we described a similar intensity peak in the oleic acid-ozone reaction system [26], which we assigned to a secondary ozonide. Therefore, the absence of any enhancement in signal intensity at 299 *m/z* upon the addition of stearic acid supports the aforementioned hypothesis, that is, that carbonyl insertion occurs at the double bond. This is supported further by our studies with MP/OL, in which the 297 *m/z* signal is clearly evident, while no significant signal is observed at 285 *m/z* or 271 *m/z*, which would correspond to oxygenation of methyl palmitate or palmitate, respectively (Fig. 1).

It should be noted that we have detected trace amounts of common fatty acids (L, LN, S, and P) in all oleic acid assayed to date. The unsaturated trace fatty acids (L and LN) could undergo a similar oxygenation to a ketone if our hypothesis is correct. Clearly evident in Fig. 2d are ion signals at 297 *m/z*, $[OL-H+O]^-$; 295 *m/z*, $[L-H+O]^-$ and a lower intensity signal at 293 *m/z*, $[LN-H+O]^-$. The signal-to-noise ($l\sigma$) for each of these ion signals is 13, 7.1 and 4.2, respectively. Note that the ion signal at 293 *m/z* may also arise from the DEA ionization of methyl linoleate while the ion signal at 295 *m/z* may arise from the methyl oleate. Therefore, these assignments are ambiguous. Recall that these ternary particles did not contain any significant amounts of the corresponding fatty acids upon generation, although as discussed above, traces of the acids could have been present, most likely through thermal degradation on the vaporization coil during heating [36]. Similarly, the 307 and 309 *m/z* are assigned to oxygenated MLN and ML. We therefore believe that the unsaturated methyl esters, as well as the corresponding fatty acids, can undergo the cycloaddition–decomposition reactions with in situ-generated Criegee intermediates to generate ketones. The oxygenation products predicted by our mechanism below that are observed in this work for all methyl esters and their corresponding acids are summarized in Table 2c.

A mechanism leading to insertion of a ketone functionality into an unsaturated methyl ester is proposed. An example of this mechanism is presented in Fig. 4 using ML as a model substrate with a general Criegee intermediate (CI). The in situ-generated Criegee intermediate is hypothesized to lose an oxygen atom after decomposition of the cycloaddition product. As explained in a prior publication [26], Criegee intermediates generated in situ probably rearrange to their corresponding carboxylic acids, which are most likely the source of DEA ions generated via PERCI. As summarized in Table 2b, 18 acids (excluding OL, L, LN) have been assigned to signals in our mass spectrum. All but three of these acids (9-oxononanoic acid, 172 u; 12-oxododec-9-enoic acid, 212 u; 15-oxopentadec-9,12-dienoic acid, 252 u) can arise through Criegee intermediates. This does not imply all

Table 2c
Abbreviated list of all novel ketones formed by the dipolarophilic reaction of an unsaturated methyl ester or fatty acid with a Criegee intermediate

| Name | Formula | MW (u) | *m/z* | Ion signal |
|---|---|---|---|---|
| LN + O | $CH_3CH_2CO(CH_2)_2CH=CHCH_2CH=CH(CH_2)_7CO_2H$ | 294 | 293 | VW, B |
| L + O | $CH_3(CH_2)_4CO(CH_2)_2CH=CH(CH_2)_7CO_2H$ | 296 | 295 | VW |
| OL + O | $CH_3(CH_2)_7CO(CH_2)_8CO_2H$ | 298 | 297 | W |
| MLN + O | $CH_3CH_2CO(CH_2)_2CH=CHCH_2CH=CH(CH_2)_7CO_2CH_3$ | 308 | 307 | VW |
| LN + 2O | $CH_3CH_2CO(CH_2)_2CO(CH_2)_2CH=CH(CH_2)_7CO_2H$ | 310 | 309 | W |
| ML + O | $CH_3(CH_2)_4CO(CH_2)_2CH=CH(CH_2)_7CO_2CH_3$ | 310 | 309 | W |
| L + 2O | $CH_3(CH_2)_4CO(CH_2)_2CO(CH_2)_8CO_2H$ | 312 | 311 | – |
| MO + O | $CH_3(CH_2)_7CO(CH_2)_8CO_2CH_3$ | 312 | 311 | – |
| MLN + 2O | $CH_3CH_2CO(CH_2)_2CO(CH_2)_2CH=CH(CH_2)_7CO_2CH_3$ | 324 | 323 | VW |
| ML + 2O | $CH_3(CH_2)_4CO(CH_2)_2CO(CH_2)_8CO_2CH_3$ | 326 | 325 | VW |
| LN + 3O | $CH_3CH_2CO(CH_2)_2CO(CH_2)_2CO(CH_2)_8CO_2H$ | 326 | 325 | VW |
| MLN + 3O | $CH_3CH_2CO(CH_2)_2CO(CH_2)_2CO(CH_2)_8CO_2CH_3$ | 340 | 339 | VW |

Note: O denotes oxygen.

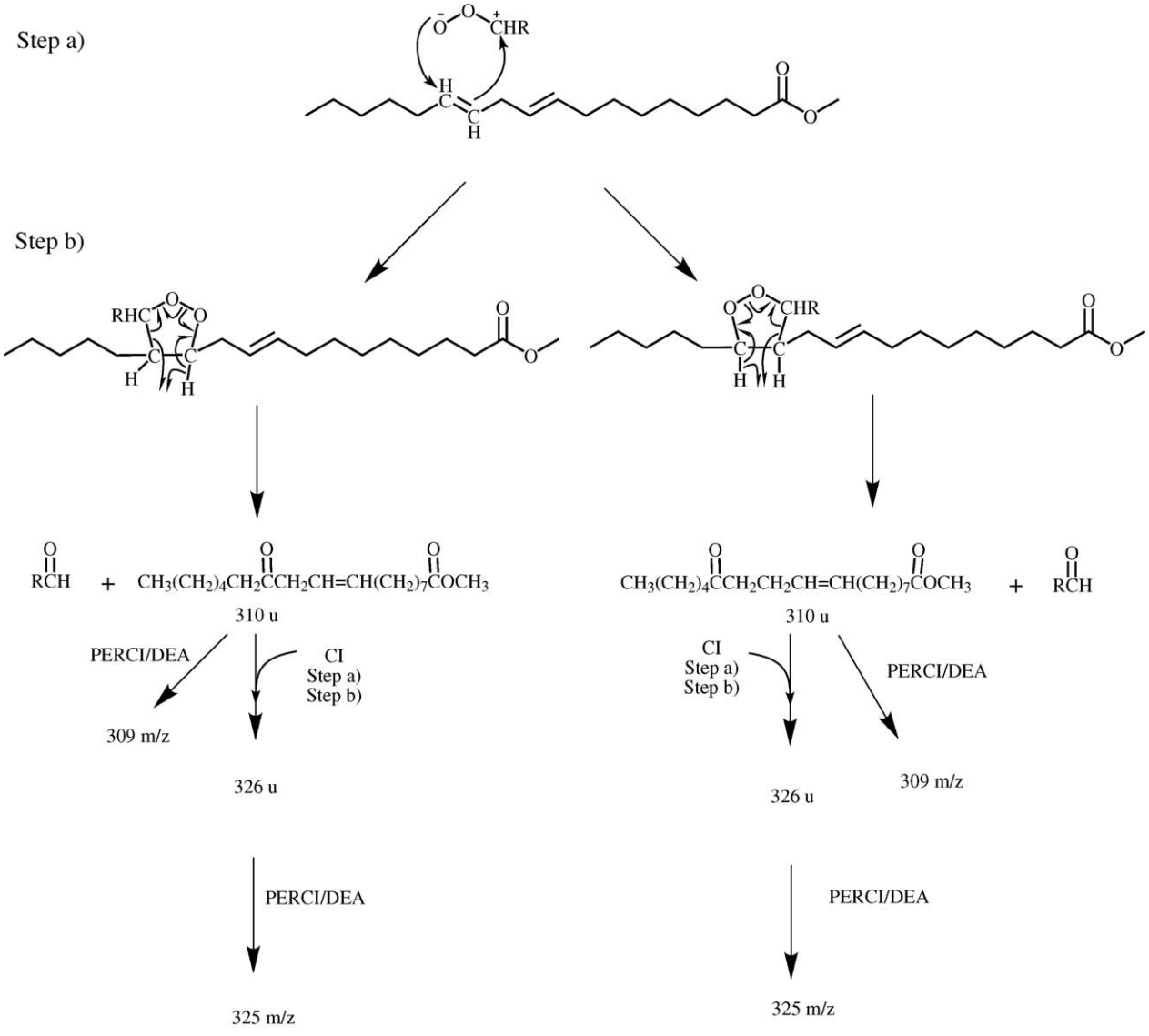


Fig. 4. Example of proposed mechanism of in situ ketone formation of an unsaturated methyl ester (ML) by an arbitrary Criegee intermediate (CI). Note that for polyunsaturated methyl esters and fatty acids, multiple cycles of the proposed cycloaddition–decomposition to ketones are possible.

of these acids arise *solely* from Criegee intermediates, however. A loss of 16 mass units due to deoxygenation of the Criegee intermediates is in accord with our model. This would imply that the acids observed that originate from Criegee intermediates would have an observed product ion at 17 mass units lower. Although there is evidence of 15 of the 16 anticipated ions predicted by this model, cases can be made for contributions to these ion signals by mechanisms independent from the one proposed in this work. Hence, the presence of these ion signals neither supports nor disproves the proposed mechanism. Their absence, on the other hand, would have disproved the proposed mechanism.

Polyunsaturated compounds, in theory, should be able to undergo multiple cycles of cycloaddition–decomposition with Criegee intermediates. In the PERCI mass spectrum of the ML/MLN/MO mixed particle (Fig. 2d), a medium-intensity signal measured at 325 *m/z* is tentatively assigned to the doubly oxygenated DEA ion of ML. For LN, the doubly and triply oxygenated DEA signals appear at 309 and 325 *m/z*, respectively. However, the 309 *m/z* could also arise, at least in part, from singly oxygenated ML, and the 325 *m/z* from the doubly oxygenated ML. The medium intensity signal at 323 *m/z* and weak 339 *m/z* signal are tentatively assigned to the doubly and triply oxygenated MLN.

## 4. Conclusion

The impact of organic aerosols, pre- and post-atmospheric processing, on the atmosphere, climate and human health remain largely uncertain [40,41]. The physical and chemical properties of organic aerosols are driven by their chemical composition and, as such, our understanding of the chemical transformations of organic particles remains a priority. For example, increases in molecular oxygen content may increase their hygroscopicity [42], thereby impacting their ability to condense water and form cloud droplets.

The work presented herein provides clear evidence of the evolution of the majority of products of a particle-gas phase heterogeneous reaction in which complex (i.e., greater than one component) particles were assayed. Of 36 primary products of ozonolysis (plus molecular ions) predicted for this ternary system, 25 were directly measured by PERCI-AMS. These products include both partial and complete ozonolysis products of the methyl esters and corresponding fatty acids.

In addition, a novel, secondary reaction was described, namely the cycloaddition of a Criegee intermediate with the double bond of an unsaturated methyl ester or fatty acid, which, upon decomposition, forms a new ketone. Multiple oxygenation cycles of polyunsaturates also is suggested from the PERCI mass spectra presented. Other secondary reactions, such as formation of secondary ozonides, as well as the chemical and physical kinetics will be described in a subsequent report.

## Acknowledgments

The authors gratefully acknowledge the financial support of the National Science Foundation (ATM-0440074), VT-EPSCoR and the National Center for Environmental Research (NCER) STAR Program, EPA (Fellowship 91615301-0).

## References

[1] A.R. Ravishankara, Science 276 (1997) 1058.
[2] M.O. Andreae, P.J. Crutzen, Science 276 (1997) 1052.
[3] F. Cousin, C. Liousse, H. Cachier, B. Bessagnet, B. Guillaume, R. Rosset, Atmos. Environ. 39 (2005) 1539.
[4] G.A. Grell, S.E. Peckham, R. Schmitz, S.A. McKeen, G. Frost, W.C. Skamarock, B. Eder, Atmos. Environ. 39 (2005) 6957.
[5] H. Herrmann, R. Wolke, K. Müller, E. Brüggemann, T. Gnauk, P. Barzaghi, S. Mertes, K. Lehmann, A. Massling, W. Birmili, A. Wiedensohler, W. Wieprecht, K. Acker, W. Jaeschke, H. Kramberger, B. Svrcina, K. Bächmann, J.L. Collett Jr., D. Galgon, K. Schwirn, A. Nowak, D. van Pinxteren, A. Plewka, R. Chemnitzer, C. Rüd, D. Hofmann, A. Tilgner, K. Diehl, B. Heinold, D. Hinneburg, O. Knoth, A.M. Sehili, M. Simmel, S. Wurzler, S. Majdik, G. Mauersberger, F. Müller, Atmos. Environ. 39 (2005) 4169.
[6] J.D. Hearn, A.J. Lovett, G.D. Smith, Phys. Chem. Chem. Phys. 7 (2005) 501.
[7] J.D. Hearn, G.D. Smith, Phys. Chem. Chem. Phys. 7 (2005) 2549.
[8] Y. Katrib, G. Biskos, P.R. Buseck, P. Davidovits, J.T. Jayne, M. Mochida, M.E. Wise, D.R. Worsnop, S.T. Martin, J. Phys. Chem. A 109 (2005) 10910.
[9] P.J. Ziemann, Faraday Discuss. 130 (2005) 469.
[10] D.A. Knopf, L.M. Anthony, A.K. Bertram, J. Phys. Chem. A 109 (2005) 5579.
[11] E. Woods III, G.D. Smith, R.E. Miller, T. Baer, Anal. Chem 74 (2002) 1642.
[12] G.B. Ellison, A.F. Tuck, V. Vaida, J. Geophys. Res. 104 (1999) 11633.
[13] R.A. Duce, V.A. Mohnen, P.R. Zimmerman, D. Grosjean, W. Cautreels, R. Chatfield, R. Jaenicke, J.A. Ogren, E.D. Pellizzari, G.T. Wallace, Rev. Geophys. Space Phys. 21 (1983) 921.
[14] G. Ketseridis, J. Hahn, R. Jaenicke, C. Junge, Atmos. Environ. 10 (1976) 603.
[15] A. Limbeck, H. Puxbaum, Atmos. Environ. 33 (1999) 1847.
[16] C. Pio, C. Alves, A. Duarte, Atmos. Environ. 35 (2001) 389.
[17] O.L. Mayol-Bracero, O. Rosario, C.E. Corrigan, R. Morales, I. Torres, V. Perez, Atmos. Environ. 35 (2001) 1735.
[18] C. Alves, C. Pio, A. Duarte, Atmos. Environ. 32 (2001) 5485.
[19] Z.G. Guo, L.F. Sheng, J.L. Feng, M. Fang, Atmos. Environ. 37 (2003) 1825.
[20] Y. Cheng, S.-M. Li, A. Leithead, P.C. Brickell, W.R. Leaitch, Atmos. Environ. 38 (2004) 5789.
[21] A. Tabazadeh, Atmos. Environ. 39 (2005) 5472.
[22] H.-M. Hung, Y. Katrib, S.T. Martin, J. Phys. Chem. A 109 (2005) 4517.
[23] J.D. Hearn, G.D. Smith, J. Phys. Chem. A 108 (2004) 10019.
[24] T. Moise, Y. Rudich, J. Phys. Chem. A 106 (2002) 6469.
[25] Y. Rudich, Chem. Rev. 103 (2003) 5097.
[26] J. Zahardis, B.W. LaFranchi, G.A. Petrucci, J. Geophys. Res. 110 (2005) D08307.
[27] Y. Katrib, S.T. Martin, H.-M. Hung, Y. Rudich, H. Zhang, J.G. Slowik, P. Davidovits, J.T. Jayne, D.R. Worsnop, J. Phys. Chem. A 108 (2004) 6686.
[28] B.W. LaFranchi, J. Zahardis, G.A. Petrucci, Rapid Commun. Mass Spectrom. 18 (2004) 2517.
[29] J. Zahardis, B.W. LaFranchi, G.A. Petrucci, Atmos. Environ. 40 (2006) 1661.
[30] J.W. Morris, P. Davidovits, J.T. Jayne, J.L. Jimenez, Q. Shi, C.E. Kolb, D.R. Worsnop, W.S. Barney, G. Cass, Geophys. Res. Lett. 29 (2002) 71-1.
[31] Y. Katrib, S.T. Martin, Y. Rudich, P. Davidovits, J.T. Jayne, D.R. Worsnop, Atmos. Chem. Phys. 5 (2005) 275.
[32] R. Criegee, Angew. Chem. Int. Edit. 14 (1975) 745.

[33] L.B. Harding, W.A. Goddard III, J. Am. Chem. Soc. 100 (1978) 7180.
[34] G. Zaikov, S. Rakovsky, Kinetics and Mechanism of Ozone Reactions with Organic and Polymeric Compounds in Liquid Phase, Nova Science Publishers, Inc., Commack, NY, 1998.
[35] B.W. LaFranchi, G.A. Petrucci, J. Am. Soc. Mass Spectrom. 15 (2004) 424.
[36] W.W. Nawar, J. Agr. Food Chem. 17 (1969) 18.
[37] J.K. Royal, G.K. Rollefson, J. Am. Chem. Soc. 63 (1941) 1521.
[38] P. Ausloos, J. Am. Chem. Soc. 80 (1957) 1310.
[39] A.L. Henne, P. Hill, J. Am. Chem. Soc. 65 (1943) 752.
[40] S. Fuzzi, M.O. Andreae, B.J. Huebert, M. Kulmala, T.C. Bond, M. Boy, S.J. Doherty, A. Guenther, M. Kanakidou, K. Kawamura, V.-L. Kerminen, U. Lohman, L.M. Russell, U. Pöschl, Atmos. Chem. Phys. Discuss. 5 (2005) 11729.
[41] M. Kanakidou, J.H. Seinfeld, S.N. Pandis, I. Barnes, F.J. Dentener, M.C. Facchini, R. van Dingenen, B. Ervens, A. Nenes, C.J. Nielsen, E. Swietlicki, J.P. Putaud, Y. Balkanski, S. Fuzzi, J. Horth, G.K. Moortgat, R. Winterhalter, C.E.L. Myhre, K. Tsigaridis, E. Vignati, E.G. Stephanou, J. Wilson, Atmos. Chem. Phys. 5 (2005) 1053.
[42] J. Sun, P.A. Ariya, Atmos. Environ. 40 (2006) 795.